

## Single-Molecule FRET Studies on Frameshifting RNA Structures of Human Immunodeficiency Virus

Heesun Hong,<sup>†,§</sup> Yang-Gyun Kim,<sup>#</sup> and Sungchul Hohng<sup>†,‡,§,\*</sup>

<sup>†</sup>Department of Physics and Astronomy, <sup>‡</sup>Department of Biophysics and Chemical Biology, <sup>§</sup>National Center for Creative Research Initiatives, Seoul National University, Seoul 151-747, Korea. \*E-mail: shohng@snu.ac.kr

<sup>#</sup>Departments of Chemistry, School of Natural Sciences, Sungkyunkwan University, Suwon 440-746, Korea  
Received February 1, 2010, Accepted February 13, 2010

**Key Words:** Human immunodeficiency virus, -1 Programmed ribosomal frameshifting, RNA pseudoknot, Single-molecule fluorescence resonance energy transfer

Correspondence between DNA sequences and its protein product is not straightforward because the genetic information can be dynamically reprogrammed during various steps of genetic decoding process. The programmed -1 ribosomal frameshifting (-1PRF) is an example of such genetic recoding mechanisms, where the reading frame of the translation machinery is shifted toward -1 direction at a predetermined position of messenger RNA.

Biochemical studies for more than last 20 years have elucidated that -1PRF occurs during the interaction of the ribosome with RNA structures, positioned 6~8 bases downstream from the frameshifting site. Except rare cases, RNA pseudoknots are the RNA structure to induce -1PRF.<sup>1</sup> In the case of HIV-1, however, it has been controversial what type of RNA structure is actually involved in -1PRF. In original studies, a basic hairpin structure positioned 7-base downstream from the slippery site (underlined in Fig. 1A) was identified as a -1PRF-inducing structure.<sup>2</sup> Subsequently, more complex RNA structures were proposed, which include a H-type pseudoknot,<sup>3</sup> the small pseudoknot,<sup>4</sup> a pseudoknot with triplex interactions,<sup>5</sup> and finally a two-stem helix structure with a central bulge.<sup>6</sup> Currently the two-stem helix structure is widely accepted as a relevant structure for -1PRF.<sup>7-9</sup> However, it is known that 8 bases are required between the A site and entrance of the ribosome on average,

suggesting that the two-stem hairpin structure with no spacer between the slippery site and the RNA structure, cannot be a relevant stimulatory structure of -1PRF. Following the same reasoning, the small pseudoknot model can be excluded from the candidate list. When -1PRF actually occurs, therefore, the lower stem of the two-stem helix should be unfolded, and a relevant structure of -1PRF might be dynamically formed during the brief period of time between the lower stem unwinding and the upper stem unwinding.

In this study, we used single-molecule fluorescence resonance energy transfer (FRET) to address what kind of structural change occurs during the unwinding process of the lower stem. Compared to the standard structure-probing and structure-function assays, single-molecule FRET technique has advantages in discriminating rare iso-forms, and identifying conformational dynamics hidden in ensemble average. For FRET studies, we designed an RNA-DNA hybrid sample as follows. The DNA strand (gray colored in Fig. 1B) was biotinylated (black circle) at the 5'-end for surface immobilization, and labeled with Cy5 (red circle) at the 3'-end for FRET measurements. The RNA strand is composed of two regions: the region complementary to the DNA strand (blue box in Fig. 1B), and the other region with RNA sequences comprising the two-stem hairpin structure (red box in Fig. 1B). For FRET measurements, the RNA strand was internally labeled with Cy3 (green circle). As clear from Fig. 1B, low FRET is expected when the two-stem hairpin is formed (on the left side of Fig. 1B), while high FRET is expected from the triplex pseudoknot structure (on the right side of Fig. 1B). The small pseudoknot would exhibit high FRET values once it is formed, but it was excluded from our consideration as explained previously. For the following discussion, the RNA-DNA hybrid sample thus formed was designated as WT. To emulate the translocation process of a ribosome, and accompanying unwinding event of the lower stem, we prepared two additional samples: Del-3 with 3 bases (orange box) removed from the 5'-end of the RNA strand, and the Del-7 with 7 bases (yellow box) removed from the 5'-end of the RNA. It is noted that the labeling position of Cy3 was designed not to perturb the formation of neither the triplex pseudoknot nor the two-stem hairpin.

Initially, we compared FRET histograms of three samples in the same buffer condition of 10 mM Tris, pH 8.0 with 150

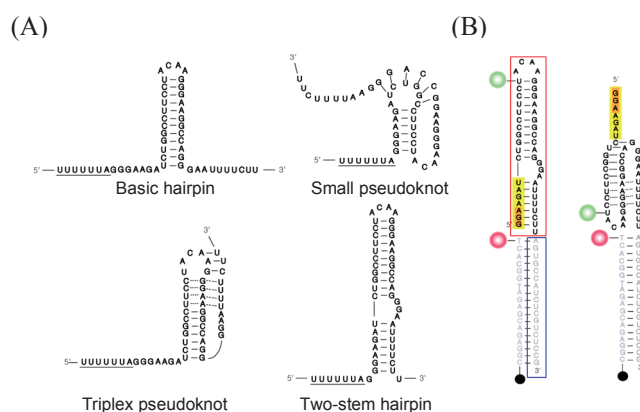


**Figure 1.** Sample design. (A) Proposed -1PRF-stimulatory RNA structures of HIV-1. (B) RNA-DNA hybrid samples of HIV-1 for single molecule FRET studies.

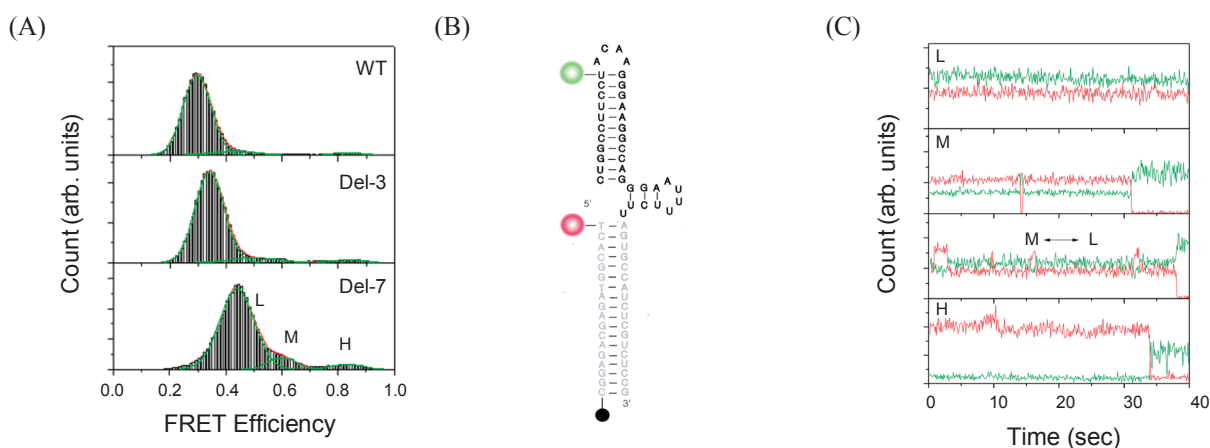
mM  $K^+$  and 10 mM  $Mg^{2+}$  (Fig. 2A). The FRET histograms of the three samples are nicely fitted to the sum of three Gaussian functions with the dominant peak at the low FRET state. The low FRET state was assigned to the two-stem hairpin structure in case of WT and Del-3, or to the basic hairpin in case of Del-7. Our observation showed that the low FRET state is still a main conformation in Del-7, which is consistent with the recent report suggesting that -1PRF stimulatory RNA structure of HIV-1 retains hairpin-like structure even when the ribosome is bound to the slippery sequence.<sup>10</sup> The fact that Del-3 and Del-7 have different low FRET values indicated that partial unfolding of the lower stem does not deconstruct the two-stem hairpin structure completely.

Even though the low FRET state is the main conformation in all three samples, our single-molecule FRET studies clearly indicate the existence of two other conformations, which are named as the middle FRET state (M), and the high FRET (H) state, respectively. The FRET efficiency of the high FRET state is what is expected from the pseudoknot structure. Even though any structure corresponding to the middle FRET state has not been predicted until now, m-fold analysis shows that this peak can be explained as the formation of a little hairpin in the

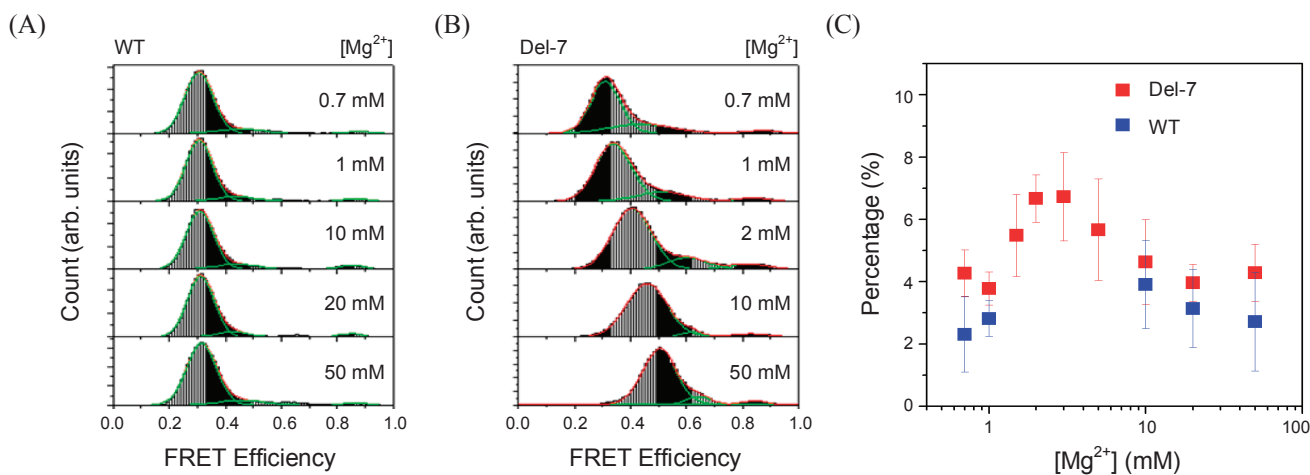
single-stranded region at the 3'-side of the upper stem, (Fig. 2B) which is exposed after the lower stem is unwound. This interpretation is also supported by the fact that the portion of the middle FRET state is increased from WT to Del-3, and to Del-7. However, there is no chance for the ribosome positioned at the slippery site to directly interact with this small hairpin, and we can safely conclude that the biological function of the middle FRET state in -1PRF is the same as that of the basic hairpin.

Fig. 2C shows representative intensity time traces of donor (green lines), and acceptor (red lines) of Del-7 molecules. Even though the high and middle FRET states are rare conformations, they are quite stable once they are formed; except rare cases which showed FRET transitions between the low FRET state and the middle FRET state, most molecules stayed in the same FRET state during observation time of  $\sim 50$  s.

Next we studied how the  $Mg^{2+}$  ions affect the relative stability of the high FRET state in WT and Del-7. It is known that the proper folding of many RNA structures requires  $Mg^{2+}$  ions as a cofactor, and the effect becomes more dramatic in compact RNA structures.<sup>11</sup> If the triplex pseudoknot of HIV-1 is a compact RNA structure as the beet western yellow virus pseudoknot, we expect a dramatic increase of the high FRET state



**Figure 2.** Heterogeneity of -1PRF-stimulatory RNA structures of HIV-1. (A) FRET histograms of WT, Del-3, and Del-7 in 10 mM Tris (pH 8.0) with 150 mM KCl, and 10 mM  $MgCl_2$ . (B) Representative intensity time traces of Cy3 (green lines) and Cy5 (red lines) of Del-7.



**Figure 3.** The effect of  $Mg^{2+}$ . (A) FRET histograms of WT at varying  $Mg^{2+}$  concentrations. (B) FRET histograms of Del-7 at varying  $Mg^{2+}$  concentrations. (C) Percentage of the high FRET state of WT (blue squares) and Del-7 (red squares) at varying  $Mg^{2+}$  concentrations.

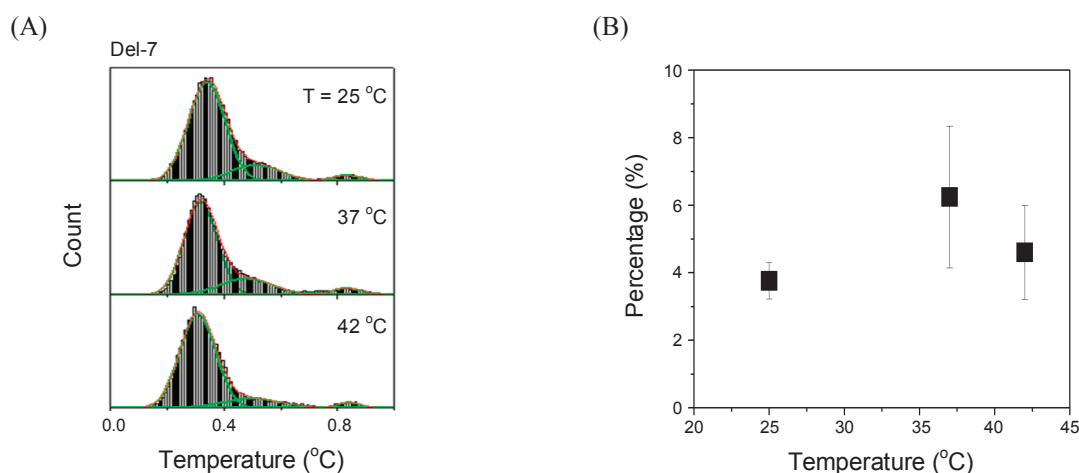


**Figure 4.** Thermal stability of the high FRET state. (A) FRET histogram of Del-7 at 25 °C, 37 °C, and 42 °C respectively in 10mM Tris (pH 8.0) with 1mM Mg<sup>2+</sup>. (B) Percentage of the high FRET state at varying temperatures.

**Table 1.** Nucleotide sequences

Name	Sequence
WT_RNA	5'-GGAAGAUCUGGCCUCCUACAAGGGAAGGCCAGGGAAUUUUCUUAGUGCCAUCUCGUCUCCG-3'
Del-3_RNA	5'-AGAUCUGGCCUCCUACAAGGGAAGGCCAGGGAAUUUUCUUAGUGCCAUCUCGUCUCCG-3'
Del-7_RNA	5'-CUGGCCUCCUACAAGGGAAGGCCAGGGAAUUUUCUUAGUGCCAUCUCGUCUCCG-3'
Com_DNA	5'-/Biotin/CGG AGA CGA GAT GGC ACT/Cy5/-3'

\*U: amine-modified U.

population at increasing Mg<sup>2+</sup> concentrations. However, the relative stability of the high FRET state is not sensitive to Mg<sup>2+</sup> ions in both WT and Del-7 (Fig. 2), suggesting that the HIV-1 pseudoknot is in loosely extended form. The gradual increase of the low FRET state in Del-7 sample can be explained by the shortening of the single-stranded RNA region due to effective screening of electrostatic repulsion of phosphate groups.

As Fig. 3C shows, the portion of the high FRET state of Del-7 is somewhat larger than that of WT in the whole range of Mg<sup>2+</sup> concentrations tested here. This observation suggests that the pseudoknot structure can be dynamically formed after the lower stem of the two-stem hairpin structure is unwound. It is probably true that the percentage of this triplex pseudoknot structure on HIV mRNAs is relatively small compared to the percentage of the two-stem hairpin structure. However, it is not assured to conclude that the pseudoknot structure is not relevant for -1PRF of HIV-1 because it is still reasonable that the triplex pseudoknot structure is much more efficient in -1PRF than the hairpin as demonstrated in many other cases.<sup>12</sup> The quantitative contribution of the triplex pseudoknot structure to overall frameshifting efficiency of HIV-1, which ranges from 5% to 10%,<sup>13-16</sup> is out of the scope of this paper.

Finally, we studied the thermal stability of the pseudoknot structure. As Fig. 4 shows, the portion of the pseudoknot structure is relatively the same at 25 °C, 37 °C, and 42 °C, indicating that the pseudoknot is stably formed at physiological temperatures.

In conclusion, we used single-molecule FRET to study the heterogeneity of -1PRF stimulatory RNA structures. As a result,

we clearly showed the triplex pseudoknot structure with high kinetic and thermal stabilities coexists with the hairpin structures in the whole range of tested salt conditions. Although majority of -1PRF may occur during the formation/unwinding process of the two-stem hairpin structure, it is still possible that the triplex pseudoknot is another relevant structure for efficient -1PRF as well. Thus, it is plausible that RNA structures contributing to -1PRF in HIV-1 may be heterogeneous.

## Experimental Section

**Sample preparation.** The RNA sequences with an amine-modified U base were purchased from Samchully. The amine-modified base was labeled with Cy3 following the protocol provided by GE Health Care. The DNA strand with Cy5 and biotin labeling was purchased from IDTDNA. All nucleotide sequences used in this work are shown in Table 1. Annealing of RNA and DNA strands was done by heating the mixture of RNA (10 μM, 3 μL), and DNA (10 μM, 1 μL) to 70 °C in 10 mM Tris (pH 8.0) with 50 mM NaCl, and slowly cooling down to 25 °C with 0.3 °C/min cooling rate. For single-molecule experiments, a narrow channel was made between a cleaned quartz microscope slides (Finkenbeiner) and a cover slip using double-sided adhesive tape. Quartz slides and cover slips were coated with polyethyleneglycol.<sup>17</sup>

For oligonucleotides immobilization, 0.2 mg/mL streptavidin was injected into the channel. After 2 minute incubation, 100 pM RNA-DNA hybrid samples were injected to the channel. The free nucleotides were washed out before starting experiments.

**Single-molecule measurements.** Images were obtained in a wide-field total-internal-reflection fluorescence microscope with 100-ms time resolution using an electron multiplying charge-coupled device (iXon DV897ECS-BV, Andor Technology) and a homemade C++ program. Diode-Pumped Solid State laser with 532-nm wavelength (Compass 215M-50, Coherent) was used to excite the molecules. The immobilized molecules were imaged in a buffer containing 10 mM Tris-HCl (pH 8.0), 0.4 mg/mL Trolox, 0.4% (w/v) glucose, 1 mg/mL glucose oxidase (Sigma), 0.02 mg/mL catalase (sigma), and specified salts.

**Acknowledgments.** This work was supported by the Korea Research Foundation Grant funded by the Korean Government (MOEHRD) (KRF-2007-314-C00185, and 313-2008-2-C00540), the World Class University (WCU) (No. R31-2009-100320) Project of the Ministry and Education, Science & Technology, and Creative Research Initiatives (Physical Genetics Laboratory, 2009-0081562) of National Research Foundation of Korea.

### References

1. Ten Dam, E. B.; Pleij, C. W.; Bosch, L. *Virus Genes* **1990**, *4*, 121.
2. Jacks, T.; Power, M. C.; Masiarz, F. R.; Luciw, P. A.; Barr, P. J.; Varmus, H. E. *Nature* **1988**, *331*, 280.
3. Le, S. Y.; Shapiro, B. A.; Chen, J. H.; Nussinov, R.; Maizel, J. V. *Genet. Anal. Tech. Appl.* **1991**, *8*, 191.
4. Du, Z.; Giedroc, D. P.; Hoffman, D. W. *Biochemistry* **1996**, *35*, 4187.
5. Dinman, J. D.; Richter, S.; Plant, E. P.; Taylor, R. C.; Hammell, A. B.; Rana, T. M. *Proc. Natl. Acad. Sci. USA* **2002**, *99*, 5331.
6. Dulude, D.; Baril, M.; Brakier-Gingras, L. *Nucleic Acids Res.* **2002**, *30*, 5094.
7. Staple, D. W.; Butcher, S. E. *J. Mol. Biol.* **2005**, *349*, 1011.
8. Gaudin, C.; Mazauric, M. H.; Traikia, M.; Guittet, E.; Yoshizawa, S.; Fourmy, D. *J. Mol. Biol.* **2005**, *349*, 1024.
9. Staple, D. W.; Butcher, S. E. *Nucleic Acids Res.* **2003**, *31*, 4326.
10. Marie-Hélène, M.; Seol, Y.; Yoshizawa, S.; Visscher, K.; Fourmy, D. *Nucleic Acids Res.* **2009**, *37*, 7654.
11. Egli, M.; Minasov, G.; Su, Li.; Rich, A. *Proc. Natl. Acad. Sci. USA* **2002**, *99*, 4302.
12. Kontos, H.; Naphine, S.; Brierley, I. *Mol. Cell. Biol.* **2001**, *21*, 8657.
13. Parkin, N. T.; Chamorro, M.; Varmus, H. E. *J. Virol.* **1992**, *66*, 5147.
14. Park, J.; Morrow, C. D. *J. Virol.* **1991**, *65*, 5111.
15. Telenti, A.; Marinez, R.; Munoz, M.; Bleiber, G.; Breub, G.; Sanglard, D. *J. Virol.* **2002**, *76*, 7868.
16. Kim, Y. G.; Maas, S.; Rich, A. *Nucleic Acids Res.* **2001**, *29*, 1125.
17. Roy, R.; Hohng, S.; Ha, T. *Nat. Methods* **2008**, *5*, 507.